Science of the Total Environment 897 (2023) 165326

Contents lists available at ScienceDirect

Science of the Total Environment

journal homepage: www.elsevier.com/locate/scitotenv

The quantitative attribution of climate change to runoff increase over the Qinghai-Tibetan Plateau

Yunfei Wang, Aizhong Ye *, Yuhang Zhang, Fan Yang

State Key Laboratory of Earth Surface Processes and Resource Ecology, Faculty of Geographical Science, Beijing Normal University, Beijing 100875, China

HIGHLIGHTS

- Annual runoff and runoff coefficient decrease from southeast to northwest on QTP.
- The annual runoff and runoff coefficient exhibit significant increasing trends.
- Precipitation variation contributes 72.08 % to the runoff increase.
- Temperature variation contributes 27.92 % to the runoff increase.

GRAPHICAL ABSTRACT

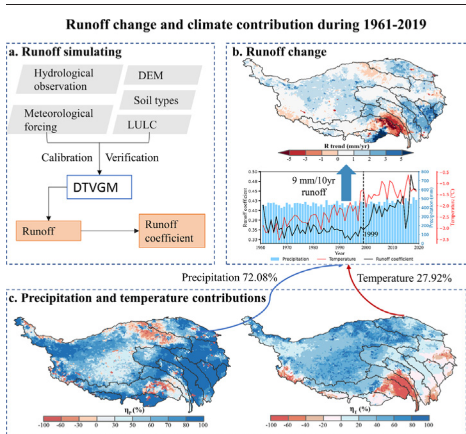

ARTICLE INFO

Editor: Ouyang Wei

Keywords:
The Qinghai-Tibetan Plateau
Runoff
Spatiotemporal changes
Climate change
Relative contribution

ABSTRACT

Runoff from the Qinghai-Tibetan Plateau, a major global water tower, is crucial to regional hydrological processes and the availability of water for a large population living downstream. Climate change, especially changes in precipitation and temperature, directly impacts hydrological processes and exacerbates shifts in the cryosphere, such as glacier and snow melt, leading to changes in runoff. Although there is a consensus on increased runoff due to climate change, it is still unclear to what extent precipitation and temperature contribute to runoff variations. This lack of understanding is one of the primary sources of uncertainty when assessing the hydrological impacts of climate change. In this study, a large-scale, high-resolution, and well-calibrated distributed hydrological model was employed to quantify the long-term runoff of the Qinghai-Tibetan Plateau, and the changes in runoff and runoff coefficient were analyzed. Furthermore, the impacts of precipitation and temperature on runoff variation were quantitatively estimated. The results found that runoff and runoff coefficient decreased from southeast to northwest, with mean values of 184.77 mm and 0.37, respectively. Notably, the runoff coefficient exhibited a significant increasing trend of 1.27 %/10 yr ($P < 0.001$), while the southeastern and northern regions of the plateau showed a declining tendency. We further showed that the warming and humidification of the Qinghai-Tibetan Plateau led to an increase in the runoff by 9.13 mm/10 yr ($P < 0.001$). And precipitation is a more important contributor than temperature across the plateau, contributing 72.08 % and 27.92 % to the runoff increase, respectively. At the basin scale, the influence of precipitation and temperature on runoff varies among basins, with the Daduhe basin and the Inner basin being the most and least influenced by precipitation, respectively. This research analyses historical runoff changes on the Qinghai-Tibetan Plateau and provides insights into the contributions of climate change to runoff.

* Corresponding author.
E-mail address: azye@bnu.edu.cn (A. Ye).

http://dx.doi.org/10.1016/j.scitotenv.2023.165326
Received 2 May 2023; Received in revised form 29 June 2023; Accepted 2 July 2023
Available online 5 July 2023
0048-9697/

1. Introduction

The Qinghai-Tibetan Plateau (QTP) is a major source of many large rivers, such as the Yangtze, Yellow, Yarlung Zangbo, Salween, Mekong, and Indus, providing a significant portion of both natural and anthropogenic water demands (Cui et al., 2023; Immerzeel and Van Beek, 2010; Yao et al., 2019a). Cryospheric elements, such as glaciers, snow, and permafrost, are widely distributed in the southeastern and western parts of the plateau (Immerzeel et al., 2020). Climate change has driven changes to the cryospheric and hydrological processes, such as the surface runoff response. The runoff coefficient, which is defined as the ratio of the runoff to the precipitation over a given period (in this study, one year) in a basin, is often used to quantify the runoff response (Merz et al., 2006; Chen et al., 2019). It is a robust index that reflects the runoff generation capacity of a basin and is widely used in hydrological research. It has been shown that the runoff coefficient is influenced by a variety of factors such as precipitation, evapotranspiration, vegetation cover, and topographic features (Chen et al., 2019; Xiong et al., 2022; Zheng et al., 2021). The research on the runoff coefficient in a basin is helpful for understanding the impact of climate change on runoff response and hydrological processes.

Runoff generation can be considered as the conversion of precipitation into runoff, which is influenced by the balance between precipitation and evapotranspiration, as well as human activities such as reservoir construction and water extraction (Zhang et al., 2001; Zheng et al., 2021). Given that human interference has little influence on the runoff owing to the high altitude of the QTP, runoff is mainly influenced by climate change (Mahmood et al., 2020; Xu et al., 2021). Over the past few decades, the QTP has undergone significant climate change, such as precipitation and temperature (Yao et al., 2019a, 2019b, 2022). For instance, the significant warming across the QTP, and precipitation increases in the northwest and decreases in the south (Yao et al., 2022; Kuang and Jiao, 2016). These changes have intensified surface hydrological cycles, influencing the cryospheric processes, such as the increasing melting of glaciers and snow, as well as permafrost degradation (Li et al., 2022a,b; Lin et al., 2019; Zhang et al., 2019b; Zhao et al., 2019). And these changes consequently lead to changes in surface runoff and affect the redistribution of freshwater resources. Understanding the response of hydrological variables such as runoff to climate change is essential for comprehending the hydrological cycle and water resources management.

Considerable advancements have been made in the study of the runoff variations on the QTP. Lutz et al. (2014) utilized a cryospheric–hydrological model to assess the runoff composition of the five major rivers (Indus, Ganges, Brahmaputra, Salween, and Mekong rivers) that originate on the QTP. They quantified the proportion of snow and glacier melt to runoff and predicted changes in runoff under climate change scenarios. Wang et al. (2021b) estimated the total river runoff of the 13 QTP rivers to be $6560 \pm 230 \times 10^8$ m^3 in 2018, which is the first estimate of its kind. Li et al. (2022a, 2022b) utilized the product water efficiency method to calculate the surface water resources of the QTP and analyzed the spatiotemporal characteristics. The results demonstrated that the annual average surface water resources have displayed a significant upward trend in the past 60 years due to the influence of climate change. Additionally, spatiotemporal analyses of runoff at basin scales such as the Yellow River source (Chen et al., 2007; Han et al., 2019; Wang et al., 2018), the Yangtze River source (Yi et al., 2021; Shi et al., 2022) and the Yarlung Zangbo (Wang et al., 2021a), indicate that climate, specifically altered precipitation and rising temperature, is the primary factor affecting runoff.

Although significant progress has been made in the study of long-term runoff dynamics, most studies have been limited to a single basin or administrative region and the comprehensive quantification of the entire QTP remains scarce. It is still unclear to what extent precipitation and temperature contribute to runoff variation, despite the fact that climate change is the primary cause of increased runoff. A comprehensive understanding of the long-term historical runoff dynamics over the QTP and an accurate estimation of the contributions of climate factors are essential for understanding how runoff responds to climate change.

The primary aims of this study are (1) to model the hydrological processes of the Qinghai-Tibetan Plateau over the past sixty years, utilizing a large-scale, well-calibrated, and fully distributed hydrological model; (2) to analyze the spatiotemporal changes of runoff and runoff coefficient using statistical methods; and (3) to estimate the relative contributions of precipitation and temperature to runoff changes.

2. Study region and data

The Qinghai-Tibetan Plateau, which has an average elevation exceeding 4000 m, is situated in the interior of the Asian continent, spanning from latitude 26°N–39°N and longitude 73°E–104°E. It is the highest and largest

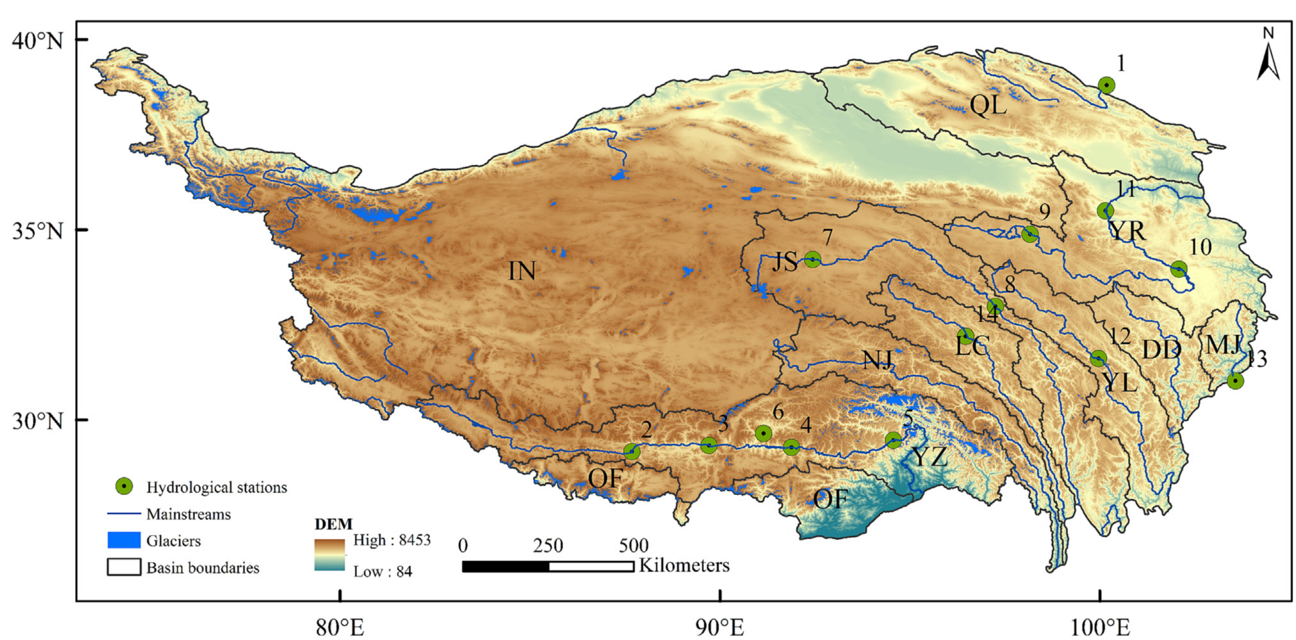

Fig. 1. The spatial distribution of the 11 basins, mainstreams, glaciers, and hydrological stations of the QTP. The 11 basins are denoted by capital letters and their corresponding full names are presented in Table 1. The numbers 1 to 14 represent the hydrological stations in these basins.

Table 1
Names and attributes of the 11 basins in the QTP.

Abbreviation	Full name	Area (km^2)	Area percentage (%)	Mean annual precipitation (mm) (1961–2019)	Mean annual temperature (°C) (1961–2019)
DD	Daduhe	61,735	2.390	898.58	0.91
IN	Inner	1,190,327	46.084	278.63	−4.33
JS	Jinshajiang	231,523	8.963	559.67	−2.03
LC	Lancangjiang	84,799	3.283	667.74	−0.09
MJ	Minjiang	25,580	0.990	964.07	2.08
NJ	Nujiang	109,103	4.224	693.18	−0.73
OF	Outflow	95,939	3.714	683.70	5.39
QL	Qilianshan	192,106	7.437	371.94	−2.48
YL	Yalongjiang	107,083	4.146	818.37	0.80
YR	Yellow River	198,042	7.667	564.37	−0.91
YZ	Yarlung Zangbo	286,729	11.101	601.49	0.89

plateau globally, covering an area of about 2.5 million km^2 and it is characterized by a diverse topography and complex environment (Yao, 2019). The climate of the plateau is complex and diverse, where the southeastern region is relatively warm and humid, while the northwestern region is cold and arid (Kuang and Jiao, 2016; Sun et al., 2015). The mean annual precipitation significantly varies in spatial distribution, decreasing from over 1000 mm in the southeast to <100 mm in the northwest (Fig. S1a). Moreover, the average annual temperature is below 0 °C in most regions, while regions with an average annual temperature above 0 °C are primarily situated at lower elevations in the southern and eastern margins of the plateau (Fig. S1b).

Accurate information about the basin is essential for precise hydrological simulation, as the basin is the key component of the hydrological model. The QTP was precisely divided into 10,937 sub-basins using a 500 m resolution digital elevation model (DEM) and subsequently integrated into 11 basins based on actual topographic features and river networks. To extract the sub-basins, we utilized the automatic extraction method for the drainage network (AEDNM). The flow direction was initially determined using the D8 method, which compares the elevation values of each pixel with those of its 8 surrounding neighboring pixels to determine the direction of flow (Jenson and Domingue, 1988). And then a step-by-step upstream search was performed from the basin outlet to establish a continuous river network. Subsequently, the sub-basins of the QTP were extracted based on the established river network (Du et al., 2017; Ye et al., 2005). The 11 basins are named as follows: the Daduhe basin (DD), the Inner basin (IN), the Jinshajiang basin (JS), the Lancangjiang basin (LC), the Minjiang basin (MJ), the Nujiang basin (NJ), the Outflow basin (OF), the Qilianshan basin (QL), the Yalongjiang basin (YL), the Yellow River basin (YR) and the Yarlung Zangbo basin (YZ). Fig. 1 displays the spatial distribution of the 11 basins, hydrological stations, glaciers, and mainstreams of the QTP, and the attributes of the 11 basins are summarized in Table 1.

The study utilized various types of data, including meteorological, hydrological, topographic, land surface, and digital elevation model (DEM) data. The details are listed in Table 2. Precipitation data was obtained from the 0.5° × 0.5° grid point dataset (V2.0) of daily precipitation on the land surface of China, and temperature data was collected from

Table 2
Data are used in this study.

Type	Variable	Description	Data sources
Meteorological	Precipitation	Daily precipitation (mm)	http://data.cma.cn/
	Temperature	Daily temperature (°C)	http://data.cma.cn/
	Glacier	Distribution and attribute	Guo et al., 2015
Land surface	LULC	Land use/cover	https://www.resdc.cn/
	Soil	Type	http://globalchange.bnu.edu.cn/research/soil2/
Hydrological	Discharge	Daily and monthly runoff discharge (m^3/s)	Hydrological yearbook and hydrological bureau
Topographical	DEM	Digital elevation model	https://www.usgs.gov/

Table 3
The attributes of hydrological stations, and the time scales and periods of hydrological data.

Station	Basin	ID	Time scale	Calibration period	Verification period
Yingluoxia	Qilianshan	1	Daily	1990–1995	1996–1999
Lazi	Yarlung	2	Daily	1980–1990	1991–1999
Nugesha	Zangbo	3	Daily	1961–1990	1991–1999
Yangcun		4	Daily	1961–1990	1991–1999
Nuxia		5	Daily	1961–1990	1991–1999
Lasa		6	Daily	1973–1990	1991–1999
Tuotuohe	Jinshajiang	7	Monthly	1961–1990	1991–1999
Zhimenda		8	Monthly	1961–1990	1991–1999
Huangheyan	Yellow River	9	Daily	1961–1990	1991–1999
Maqu		10	Monthly	1961–1990	1991–1999
Tangnaihai		11	Daily	1961–1990	1991–1999
Ganzi	Yalongjiang	12	Daily	1980–1990	1991–1999
Zipingpu	Minjiang	13	Daily	1961–1990	1991–1999
Xiangda	Lancangjiang	14	Monthly	1961–1990	1991–1999

meteorological stations. Glacier data was sourced from the Second Glacier Inventory Dataset of China (Version 1.0) (Guo et al., 2015). The DEM, land use/cover, and soil type data with a spatial resolution of approximately 1 km were used to characterize the spatial variability of the land surface and to set up the hydrological model. Daily and monthly discharge records from 14 hydrological stations covering a long-term period, primarily between 1961 and 1999, were used to calibrate and verify the model. The relevant summary of these discharge records is presented in Table 3.

3. Methods

Fig. 2 provides an overview of this study. Firstly, we set up, calibrated, and verified the Distributed Time-Variant Gain Hydrological Model (DTVGM) from 1961 to 2010. Subsequently, we simulated the long-term runoff of the QTP and calculated the runoff coefficient. Secondly, we divided the study period into two periods based on the results of the mutation test for the runoff coefficient and systematically analyzed the spatiotemporal changes in runoff and runoff coefficient. Finally, we quantitatively estimated the relative contributions of precipitation and temperature to changes in runoff.

3.1. Trend analysis based on linear regression

The linear regression and the F-significance test were utilized to detect and analyze the long-term trends of the runoff and runoff coefficient during 1961–2019. Linear regression is a statistical method that models the association between the independent variable $X = \{x_1, x_2, \ldots, x_n\}$ and the dependent variable $Y = \{y_1, y_2, \ldots, y_n\}$, and the F-test is used to evaluate the significance of the trend obtained from linear regression (Box, 1953). The calculation for linear regression is expressed by Eq. (1):

$$Y = \beta_0 + \beta_1 X \tag{1}$$

The parameters β_0 and β_1 are usually determined using the least squares method to achieve the best fit to the data, calculated as follows:

$$\beta_1 = \frac{\sum_{i=1}^{i=n} x_i \cdot y_i - \frac{1}{n}\sum_{i=1}^{i=n} x_i \cdot \sum_{i=1}^{i=n} y_i}{\sum_{i=1}^{i=n} (x_i - \bar{x})^2} \tag{2}$$

$$\beta_0 = \bar{y} - \beta_1 \bar{x} \tag{3}$$

$$\bar{x} = \frac{1}{n}\sum_{i=1}^{n} x_i \quad \bar{y} = \frac{1}{n}\sum_{i=1}^{n} y_i \tag{4}$$

where $\bar{x}$ is the mean observed value; $\bar{y}$ is the mean predictor variable at which the observations were taken. The coefficient β_1 denotes the change degree of Y along with X.

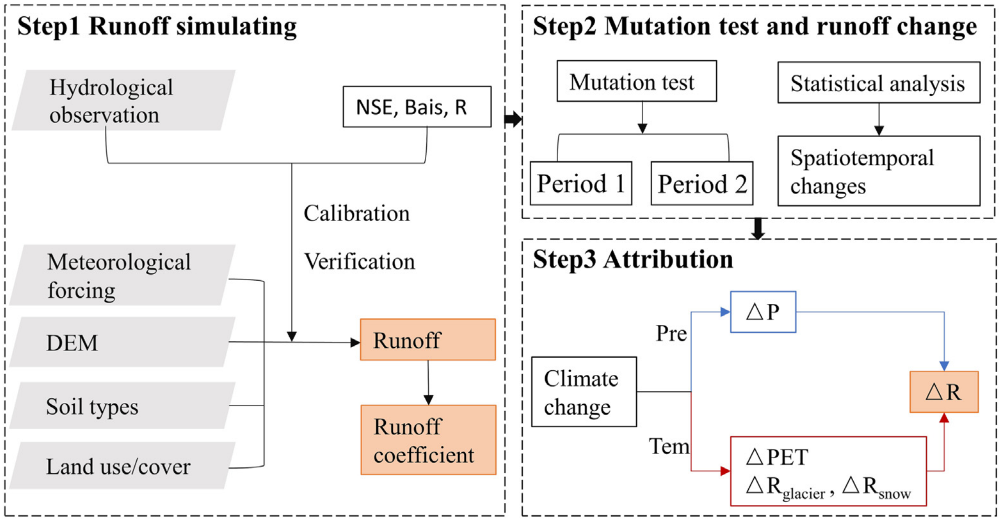

Fig. 2. Flowchart of this study. The Nash-Sutcliffe efficiency (NSE), relative bias (Bais), and correlation coefficient (r) were used as evaluation metrics. The period 1 represents 1961–1999 and the period 2 represents 2000–2019. The variables used in this study include precipitation (Pre), temperature (Tem), precipitation change (ΔP), potential evapotranspiration change (ΔPET), glacier melt change ($\Delta R_{glacier}$), snow melt change (ΔR_{snow}), and runoff change (ΔR).

3.2. Variation point analysis based on Pettitt test

The Pettitt test, a non-parametric method, is commonly used to identify abrupt changes in hydroclimatic variables, such as runoff and precipitation (Pettitt, 1979). A mutation year indicates that the variable has changed statistically around that year (Petrone et al., 2010; Mallakpour and Villarini, 2016; Zhang et al., 2019a).

3.3. Distributed time-variant gain hydrological model

The Distributed Time-Variant Gain Hydrological Model (DTVGM) that was first proposed by Xia et al. (2003) is used to simulate the long-term runoff of the QTP. The DTVGM is a large-scale, high-resolution model that uses a daily time step with 10,937 sub-basins in this study. Moreover, it is a fully distributed model and has been successfully applied in various basins (Xia et al., 2005; Ye et al., 2010; Zhang et al., 2021). The DTVGM can simulate all major hydrological and cryospheric processes, including the glacier and snow melt.

The DTVGM calculates evapotranspiration, soil water content, soil flow, base flow, glacier melt, snow melt, and surface runoff for each sub-basin. The kinematic wave model is used for routing calculating (Ye et al., 2013). The water balance equation for each sub-basin is as follows:

$$P_i + W_i + R_{snow} + R_{glacier} = W_{i+1} + Rs_i + E_i + Rss_i + Rg_i \tag{5}$$

where P represents precipitation (mm); W represents soil moisture content (mm); R_{snow} represents snow melt (mm); $R_{glacier}$ represents glacier melt (mm); Rs represents surface runoff (mm); E represents evapotranspiration (mm); Rss represents subsoil water (mm); Rg represents groundwater runoff (mm); i represents the number of periods.

The calculation of surface runoff at each sub-basin is as follows:

$$\text{Rs} = g_1\left(\frac{AW_u}{WM_u \cdot C}\right)^{g_2} \cdot \left(P + R_{snow} + R_{glacier}\right) \tag{6}$$

where Rs is surface runoff at the sub-basin (mm); AWu is the upper soil moisture at the sub-basin (mm); WM_u is the upper saturated soil moisture (mm); P is precipitation (mm); R_{snow} is snow melt (mm); $R_{glacier}$ is glacier melt (mm); g_1 and g_2 are parameters ($0 < g_1 < 1$, $0 < g_2$); g_1 is the runoff coefficient when the soil is saturated; g_2 is the soil moisture parameter; C is the land cover parameter; R_{snow} and $R_{glacier}$ are calculated using the degree-day factor model with the following formula:

$$R_{snow,glacier} = \begin{cases} DDF_{snow,glacier} \cdot (T_{av} - T_{mlt}), T_{av} \geq T_{mlt} \\ 0, T_{av} < T_{mlt} \end{cases} \tag{7}$$

where, $R_{snow,glacier}$ is snow or glacier melt (mm); $DDF_{snow,glacier}$ is the degree-day factor for snow or glacier (mm·°C^{-1}·d^{-1}); T_{av} is the daily mean temperature (°C); T_{mlt} is the critical temperature of snow or glacier melting (°C).

The model performance is evaluated by three metrics: Nash-Sutcliffe efficiency (NSE), correlation coefficient (r), and relative bias (Bias). Higher values of the NSE and r indicate better model performance, whereas lower values of the Bais indicate better model performance. In the calibration process, we aimed for a good combined performance of the NSE, r, and Bias. The NSE, r, and Bias are calculated as follows:

$$\text{NSE} = 1 - \frac{\sum (Q_s - Q_o)^2}{\sum (Q_o - \overline{Q_o})^2} \tag{8}$$

$$\text{r} = \frac{\sum (Q_s - \overline{Q_s})(Q_o - \overline{Q_o})}{\sqrt{\sum (Q_s - \overline{Q_s})^2 \sum (Q_o - \overline{Q_o})^2}} \tag{9}$$

$$Bias = \left(\frac{\sum Q_s}{\sum Q_o} - 1\right) \times 100\% \tag{10}$$

where Q_s represents the simulated value (m^3/s); Q_o represents the observed value (m^3/s); $\overline{Q_o}$ represents the average observed value (m^3/s); $\overline{Q_s}$ represents the average simulated value (m^3/s).

3.4. Attribution of the runoff change

The runoff coefficient, which reflects the relationship between precipitation and runoff in the basin, is defined as the ratio of runoff depth to the precipitation depth during a given period (a year in this study), and is calculated using Eq. (11):

$$\text{Rc} = \frac{R}{P} \tag{11}$$

where R is the runoff (mm), and P is the precipitation (mm).

The annual runoff difference is used to quantify the magnitude of runoff change on the QTP, and is calculated using Eq. (12). The impact of precipitation and temperature on runoff change can be calculated using Eqs. (13)–(15):

$$R_{change} = \frac{R_2 - R_1}{R_1} \cdot 100\% \tag{12}$$

$$\Delta Q_t = \Delta Q_P + \Delta Q_T = Q_{obs} - Q_{base} \tag{13}$$

$$\Delta Q_P = Q_{obs} - Q_{sim} = Q_{obs2} - P_2 \cdot RC_1 \tag{14}$$

$$\Delta Q_T = Q_{sim} - Q_{base} = P_2 \cdot RC_1 - Q_{obs1} \tag{15}$$

where, R_{change} is the runoff difference between the two periods; R_1 is the mean annual runoff of the period 1; R_2 is the mean annual runoff of the period 2; ΔQ_t is the total runoff change; ΔQ_P is the runoff change due to precipitation; ΔQ_T is the runoff change due to temperature; Q_{sim} represents the simulated runoff calculated by precipitation and runoff coefficient; Q_{obs} represents the actual runoff, which is directly from the results of the hydrological model; Q_{obs1} represents the runoff of the period 1; Q_{obs2} represents the runoff of the period 2; Q_{base} represents the runoff of the period 1, which is directly from the results of the hydrological model; P_2 is the precipitation of the period 2; RC_1 is the runoff coefficient of the period 1.

The relative contributions of precipitation (η_P) and temperature (η_T) to runoff change can be quantified using Eqs. (16) and (17). A positive value of η indicates that a change in precipitation (temperature) increases runoff, whereas a negative value implies that a change in precipitation (temperature) leads to a decrease in runoff.

$$\eta_P = \frac{\Delta Q_P}{|\Delta Q_T| + |\Delta Q_P|} \cdot 100\% \tag{16}$$

$$\eta_T = \frac{\Delta Q_T}{|\Delta Q_T| + |\Delta Q_P|} \cdot 100\% \tag{17}$$

4. Results

4.1. Model calibration results

Fig. 3 displays the observed and simulated discharge as well as precipitation for 14 hydrological stations during both the calibration and validation periods. Owing to data availability constraints of observed discharge, the selected period varies slightly across hydrological stations, mostly from 1961 to 1999.

Most of the hydrological stations have NSE values exceeding 0.7 during both calibration and verification periods. For example, the NSE values during the verification period are 0.89, 0.87, and 0.85 for Maqu, Xiangda, and Tangnaihai, respectively (Table 4). Additionally, all correlation coefficients for calibration and verification periods are above 0.7, with some stations having correlation coefficients above 0.9. Moreover, all Bias values were within 10 %. The agreement between simulated and observed discharge is good, and the relationship between discharge and precipitation is found to be relatively stable. These results suggest that the hydrological model has sufficient accuracy to achieve long-term runoff simulations.

4.2. Spatial variations of runoff and runoff coefficient

Fig. 4 shows the spatial distribution of the mean annual runoff and runoff coefficient on the QTP during 1961–2019. The mean annual runoff ranges from 1.76 mm (e.g., desert areas in the Inner basin) to 1605.97 mm with a mean value of 184.77 mm. The runoff spatial pattern shows a decreasing trend from southeast to northwest (Fig. 4a). Similarly, the spatial distribution of precipitation is also high in the southeast and low in the west of QTP (Fig. S1a). The regions with high runoff are primarily distributed in the southeastern and eastern areas of the plateau, such as the downstream of the YZ and the NJ. Meanwhile, the low runoff areas are widespread in the central and western parts of the plateau, which are arid regions with scarce precipitation.

Fig. 4b shows the spatial distribution of the mean annual runoff coefficient across the QTP during 1961–2019. The mean annual runoff coefficient ranges from 0.02 (e.g., in the northwestern desert region of the QTP) to 0.94, with a mean value of 0.37. Similar to the runoff, the runoff coefficient also exhibits a spatial pattern of high in the southeast and low in the northwest. The regions with high runoff coefficients are mainly located in the southern and eastern regions of the plateau, as well as the QL in the north, indicating a significant capacity for surface runoff conversion in these areas. Conversely, the northwestern and central regions of the plateau, which are mainly dry sandy areas with little rainfall and runoff, have low values of runoff coefficient. In particular, the annual runoff coefficient exceeds 0.6 along the southern border of the QTP, the NJ, and the JS, while most of the northwestern part of the plateau exhibits a runoff coefficient below 0.2.

4.3. Temporal changes of runoff and runoff coefficient

4.3.1. Variation points in runoff coefficient

We applied the Pettitt test to detect variation points in the annual runoff coefficient series across the QTP and 11 basins. The results showed that the runoff coefficient of the QTP experienced a variation point in the year 1999, and the 11 basins also experienced variation points around the year 2000 (Fig. 5). Consequently, the year 2000 was used as the boundary to split the period 1961–2019 into two periods, namely the reference period (1961–1999, referred to as the first period, or period 1) and the change period (2000–2019, referred to as the second period, or period 2). The numerical subscripts 1 and 2 are used to differentiate the first and second periods respectively. For instance, the average annual runoff coefficient for the first period of 1961–1999 is represented as RC_1.

4.3.2. Trends of runoff and runoff coefficient

Fig. 5 shows the interannual variations of the runoff coefficient, precipitation, and temperature across the QTP and 11 basins from 1961 to 2019. The mean annual runoff and runoff coefficient of the QTP show significant increasing trends with rates of 9.13 mm/10 yr ($P < 0.001$) and 1.27 %/10 yr ($P < 0.001$), respectively. Additionally, the QTP displays significant increasing trends in precipitation and temperature, with rates of 7.65 mm/10 yr ($P < 0.001$) and 0.37 °C/10 yr ($P < 0.001$), respectively. The runoff coefficients of basins demonstrate increasing trends, but the rate of increase varies. The MJ and the YL show the highest rate of increase, with rates of 2.40 %/10 yr ($P < 0.001$) and 2.35 %/10 yr ($P < 0.001$), respectively. Both the QTP and basins exhibit a highly significant increasing trend in temperature ($P < 0.001$), although the magnitude of the increase varies. However, the basins show both increasing and decreasing trends in precipitation, with the increasing trend dominating. At the basin scale, the NJ showed a significantly decreasing trend of 15.44 mm/10 yr ($P < 0.05$), whereas the LC and the YZ showed non-significant decreasing trends of −3.81 mm/10 yr and − 3.05 mm/10 yr, respectively.

Fig. 6 displays the runoff and runoff coefficient of the QTP and 11 basins for the years 1961–2019 and the two periods. At the basin scale, the median value of the mean annual runoff is highest in the MJ, the NJ, and the DD, by 568.27 mm, 365.93 mm, and 359.20 mm, respectively. Conversely, the median value of the mean annual runoff is lowest in the IN, the QL, and the JS, by 79.29 mm, 121.96 mm, and 129.65 mm, respectively. The most notable change between the two periods occurred in the YL, where the median value increased from 280.92 mm to 389.92 mm. The runoff coefficient also exhibits differences at the basin scale. The MJ, the NJ, the LC, and the YZ have the highest runoff coefficients, with median values of 0.63, 0.56, 0.51, and 0.51, respectively. The JS and the IN have the lowest runoff coefficients, with values of 0.24 and 0.31, respectively. Similar to the runoff, the YL has the most prominent change in the runoff coefficient, with

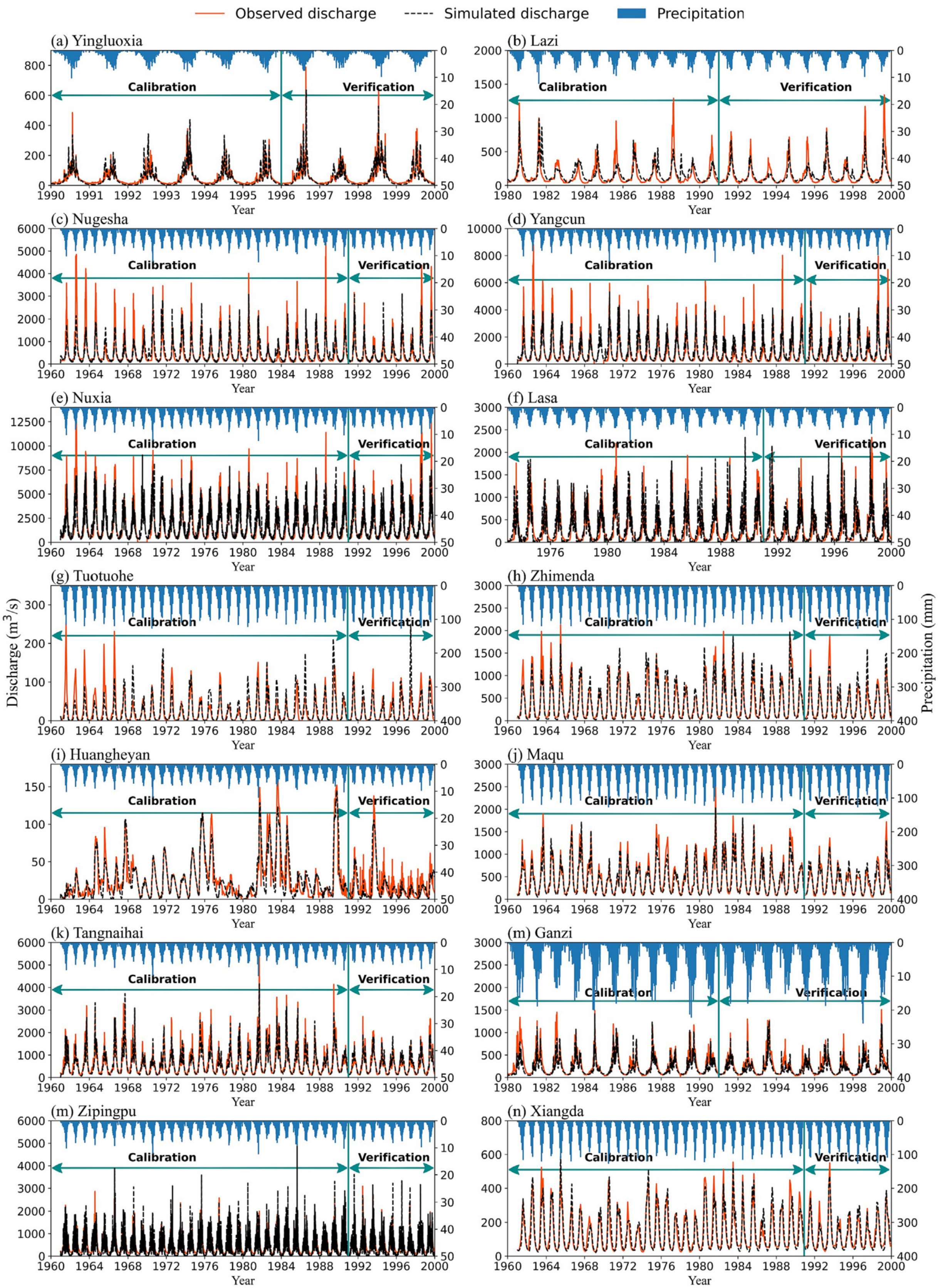

Fig. 3. Long-term hydrographs for calibration and verification periods at 14 hydrological stations.

median values of 0.37 and 0.50 in periods 1 and 2, respectively. Comparing the two periods, both the QTP and the 11 basins have higher runoff and runoff coefficient in period 2 than in period 1.

Fig. 7 shows the spatial pattern of the interannual rate of the runoff and runoff coefficient across the QTP during 1961–2019. The interannual trend of annual runoff ranges from −10.10 mm/yr (e.g., downstream of the YZ)

Table 4
Model calibration and verification for runoff simulation at 14 hydrological stations.

Station	Calibration				Verification			
	Period	NSE	r	Bias (%)	Period	NSE	r	Bias (%)
Yingluoxia	1990–1995	0.70	0.90	0.80	1996–1999	0.70	0.87	3.23
Lazi	1980–1990	0.50	0.72	9.36	1991–1999	0.69	0.86	9.11
Nugesha	1961–1990	0.69	0.84	−1.40	1991–1999	0.80	0.90	1.94
Yangcun	1961–1990	0.73	0.86	5.00	1991–1999	0.81	0.91	2.36
Nuxia	1961–1990	0.71	0.85	−4.00	1991–1999	0.76	0.88	−6.23
Lasa	1973–1990	0.60	0.81	6.00	1991–1999	0.64	0.82	2.17
Tuotuohe	1961–1990	0.55	0.76	−1.00	1991–1999	0.55	0.79	1.15
Zhimenda	1961–1990	0.86	0.93	−2.00	1991–1999	0.81	0.91	3.25
Huangheyan	1961–1990	0.87	0.93	−2.00	1991–1999	0.70	0.86	1.09
Maqu	1961–1990	0.90	0.96	−9.00	1991–1999	0.89	0.95	−0.24
Tangnaihai	1961–1990	0.88	0.95	−9.00	1991–1999	0.85	0.92	1.10
Ganzi	1980–1990	0.72	0.90	−9.60	1991–1999	0.75	0.91	−9.34
Zipingpu	1961–1990	0.79	0.89	−4.00	1991–1999	0.51	0.85	−9.48
Xiangda	1961–1990	0.85	0.92	0.00	1991–1999	0.87	0.94	−0.66

to 11.34 mm/yr. There is an overall increasing trend of the runoff, with a mean value of 0.89 mm/yr. And the increasing tendencies are found in all 11 basins, although the magnitudes of the trends vary. The DD and the MJ have the highest increasing trends with median values of 2.73 mm/yr and 2.20 mm/yr, respectively, whereas the NJ has the lowest with a median value of 0.11 mm/yr (Fig. S2a). However, the southwestern border and northern areas of the QTP, as well as the downstream of the YZ and the NJ, show decreasing trends.

The trend of the annual runoff coefficient varies from −1.74 %/yr (e.g., downstream of the YZ) to 1.18 %/yr (Fig. 7b). The annual runoff coefficient across the QTP also shows an overall increasing trend with a mean value of 0.13 %/yr. At the basin scale, the runoff coefficient all show increasing trends (the median of the runoff coefficient trend is all greater than zero). Among them, the DD, the YL, and the MJ have the most significant increase, with median values of 0.25 %/yr, 0.25 %/yr, and 0.22 %/yr, respectively, while the YZ has the lowest increase with median value of 0.07 %/yr (Fig. S2b). However, in the north-central QTP and the downstream of the YZ and the NJ, the runoff coefficient show decreasing trends, indicating that the transformation of precipitation into surface runoff has weakened.

4.4. Attribution of the runoff increase

Fig. 8 shows the spatial pattern of the magnitude of runoff variation across the QTP over the two periods. The variation ranged from −38.60 % to 606.27 % (notably, desert areas in the northwestern QTP have the highest magnitude of runoff variation). Due to the low annual runoff in desert areas, even a slight change in the runoff can result in a variation several times higher than the original value. As an example, if R1 = 2 mm, and R2 = 8 mm, R_{change} would be 300 %. At the basin scale, the runoff increase rate varies. Among them, the IN and the QL have the largest runoff change of 42.14 % and 41.64 %, respectively. These two regions have a very low annual runoff, and a slight change in runoff can lead to significant variability, especially in the IN. In contrast, the NJ has the lowest variation in runoff at only 8.98 %.

Fig. 9 shows the spatial pattern of relative contributions of precipitation and temperature to runoff change, and Fig. 10 illustrates the contributions at the basin scale. Precipitation is a more important contributor than temperature across the QTP, contributing 72.08 % and 27.92 % to the runoff change, although the contribution has a spatial difference. At the basin scale, the degree of influence by precipitation and temperature varies. Among them, the IN is almost equally influenced by precipitation and temperature, while the DD, the YR, and the YL are dominated by the influence of precipitation.

The η_P is positive in most regions, suggesting that precipitation leads to an increase in runoff in the majority of the plateau. However, in the downstream YZ, the downstream NJ, the northeastern IN, and the southwestern QL, η_P is negative, which suggests that precipitation has resulted in a decrease in runoff (Fig. 9a). This can be attributed to the significant and continuous decrease in precipitation over the past 60 years in these regions (Fig. S3a). The median η_P for 11 basins is positive (Fig. 10), with the highest in the DD ($\overline{\eta_P}$ = 99.03 %) and the lowest in the IN ($\overline{\eta_P}$ = 54.25 %), suggesting that changes in precipitation increase runoff at the basin scale.

The relative contribution of temperature to runoff change varies spatially, as shown in Fig. 9b. Specifically, the η_T is negative along the southern and eastern border of the QTP, the downstream NJ, and the YZ, indicating that the temperature change decreases the runoff. At the basin scale, the effect of temperature on runoff is both positive and negative. In the DD, the LC, the MJ, the NJ, the OF, and the YL, the values of $\overline{\eta_T}$ are −0.97 %, −3.99 %, −10.7 %, −30.97 %, −9.65 %, and −3.99 %, respectively, implying that temperature decreases runoff. Conversely, the $\overline{\eta_T}$ of the IN, the JS, the QL, the YR, and the YZ are positive, indicating that temperature leads to an increase in runoff. Additionally, the basins with the highest and lowest influence of temperature are the IN and the DD, with values of $\overline{\eta_T}$ of 45.75 % and −0.97 %, respectively.

5. Discussion

The QTP has experienced significant climate change, such as precipitation change and warming. The spatial pattern of precipitation change on the QTP is variable, with some regions experiencing an increase, while the eastern and southern parts of the plateau are becoming drier (Gao et al., 2015; Kuang and Jiao, 2016; Yao et al., 2022). The studies have shown a significant increase in temperature on the QTP, with a warming rate ranging from 0.16 to 0.67 °C/10 yr (Peng et al., 2021; Han et al., 2019). Climate change not only directly influences the surface runoff response, but also indirectly affects the runoff through glacier and snow melt (Yao et al., 2012; Zhao et al., 2019). Numerous studies have investigated the dynamic changes and attribution of the historical runoff on the QTP in the context of climate change. Surface water resources on the QTP significantly increased at a rate of 388.85 × 10^8 m^3/10 yr from 1956 to

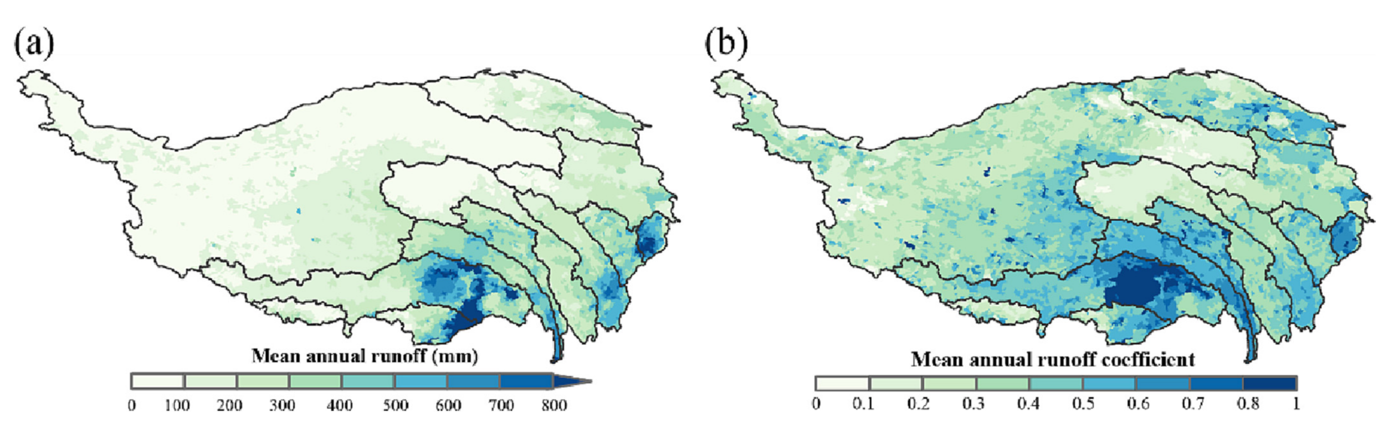

Fig. 4. Spatial distribution of the mean annual runoff (a) and runoff coefficient (b) of the QTP during 1961–2019.

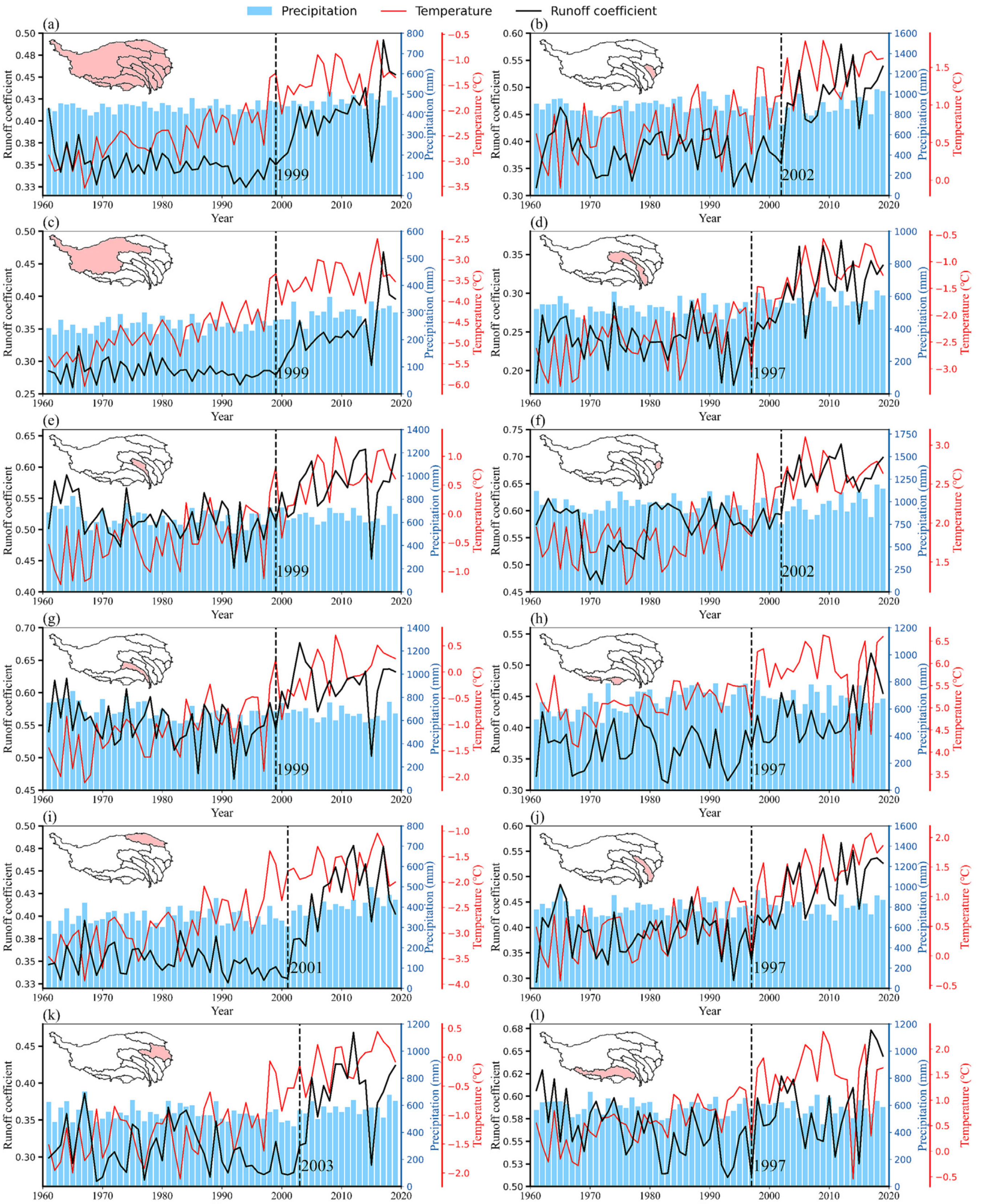

Fig. 5. Interannual changes of mean annual runoff coefficient, precipitation, and temperature of the QTP and 11 basins during 1961–2019. The blue bars indicate the precipitation, the black line indicates the runoff coefficient, the red line indicates temperature and the vertical black dashed line indicates the variation point year of the runoff coefficient. The shadow region of inserted the QTP boundary on the top-left corner denotes the geographical location of each basin. (a)–(l), the QTP (a), the Daduhe basin (b), the Inner basin (c), the Jinshajiang basin (d), the Lancangjiang basin (e), the Minjiang basin (f), the Nujiang basin (g), the Outflow basin (h), the Qilianshan basin (i), the Yalongjiang basin (j), the Yellow River basin (k) and the Yarlung Zangbo basin (l).

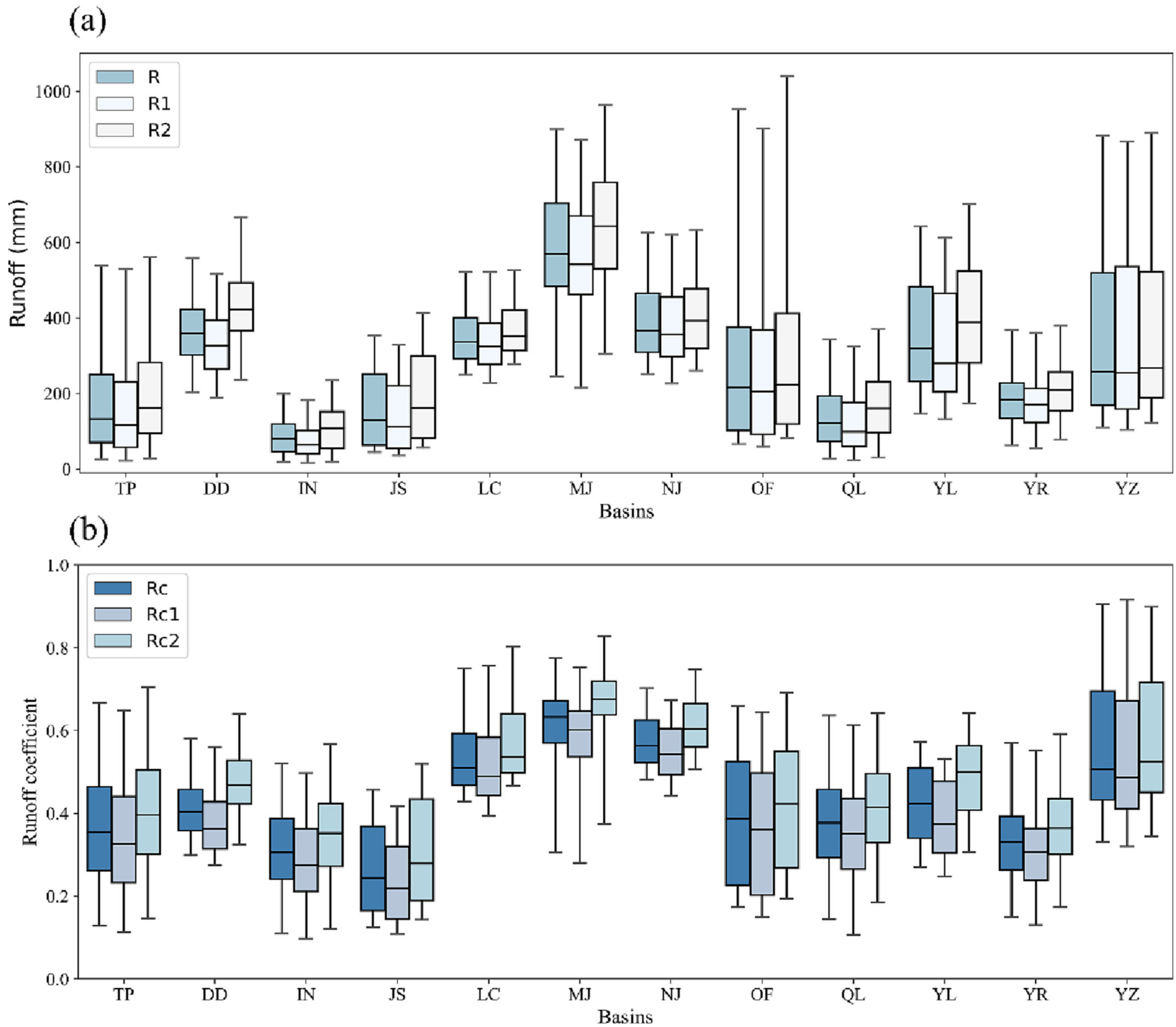

Fig. 6. Runoff (a) and runoff coefficient (b) of the QTP and 11 basins during 1961–2019. R represents the mean annual runoff (mm) during 1961–2019, R1 represents the mean annual runoff (mm) of period 1 (1961–1999) and R2 represents the mean annual runoff (mm) of period 2 (2000–2019). Rc represents the mean runoff coefficient during 1961–2019, Rc1 represents the mean runoff coefficient of period 1 (1961–1999) and Rc2 represents the mean annual runoff coefficient of period 2 (2000–2019). The 11 basins are the Daduhe basin (DD), the Inner basin (IN), the Jinshajiang basin (JS), the Lancangjiang basin (LC), the Minjiang basin (MJ), the Nujiang basin (NJ), the Outflow basin (OF), the Qilianshan basin (QL), the Yalongjiang basin (YL), the Yellow River basin (YR) and the Yarlung Zangbo basin (YZ).

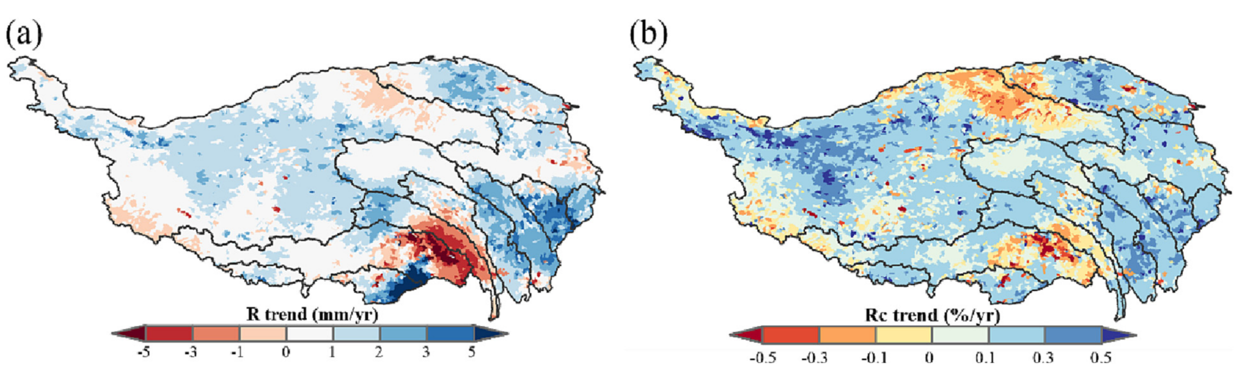

Fig. 7. Spatial pattern of runoff (a) and runoff coefficient (b) trends on the TP during 1961–2019.

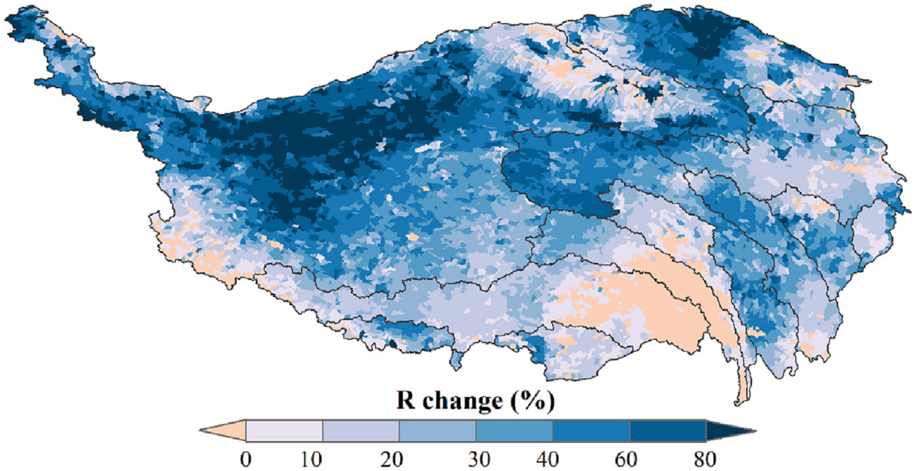

Fig. 8. Spatial distribution of the magnitude of change in mean annual runoff over the two periods.

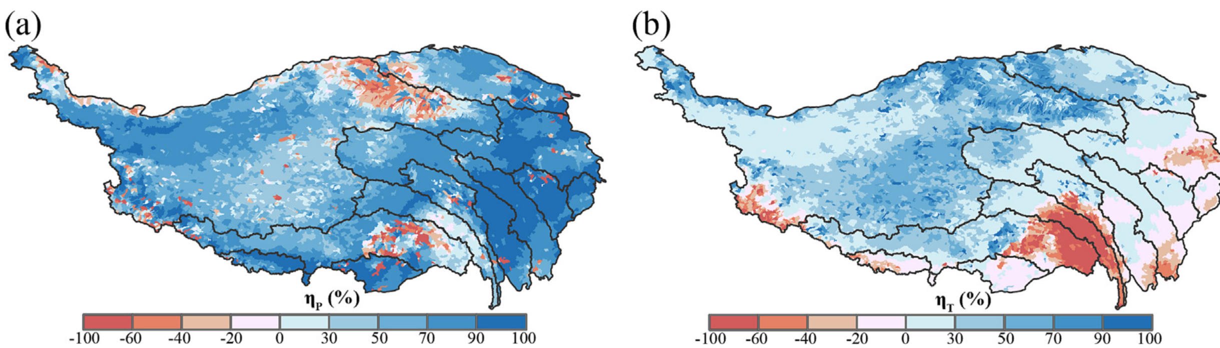

Fig. 9. Spatial distribution of the relative contributions of precipitation η_P (a), and temperature η_T (b) to runoff change.

2018 according to Li et al. (2022a, 2022b). Our study also found a substantial increase in runoff, at a rate of 9.13 mm/10 yr from 1961 to 2019 (P < 0.001), consistent with the results of Li et al. According to Wang et al. (2018), an analysis of the runoff changes in the Yellow River source using the Budyko framework revealed that precipitation is the primary factor influencing runoff variation. And our findings are consistent with earlier research (Li et al., 2022a, 2022b; Liu et al., 2020), as we observed a decrease in runoff from the southeastern to northwestern regions of the plateau, while a significant increase occurred over the decades.

The attribution results indicate that precipitation is a more important contributor than temperature across the QTP, with relative contributions of 72.08 % and 27.92 %, respectively. Changes in precipitation can directly influence the surface runoff generation process, leading to significant increases or decreases in surface runoff. As shown in Fig. S4a, the decreasing runoff in the downstream NJ and YZ is consistent with the decline in precipitation. Warming can affect the surface evapotranspiration processes and lead to the melting of glaciers and snow, indirectly influencing surface runoff. With increasing temperatures, there is an increase in water

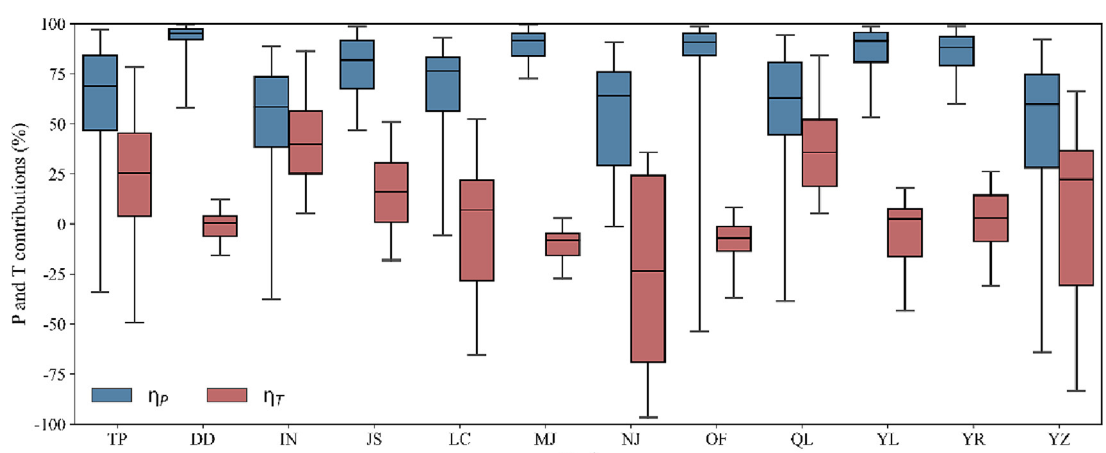

Fig. 10. Relative contributions of precipitation and temperature to runoff change in the QTP and 11 basins. The 11 basins are the Daduhe basin (DD), the Inner basin (IN), the Jinshajiang basin (JS), the Lancangjiang basin (LC), the Minjiang basin (MJ), the Nujiang basin (NJ), the Outflow basin (OF), the Qilianshan basin (QL), the Yalongjiang basin (YL), the Yellow River basin (YR) and the Yarlung Zangbo basin (YZ).

evapotranspiration from land surfaces, resulting in a deduction of surface runoff. Conversely, warming leads to more glaciers and snow melt, which increases the runoff. Research studies have shown that glacier melting contributes to only a small proportion of runoff (Han et al., 2019; Lutz et al., 2014; Wang et al., 2021a, 2021b), indicating that warming has a minimal influence on the increase in runoff. Although the temperature has a lesser influence on runoff variation compared to precipitation, it plays a regulatory role in runoff change on the QTP.

There are also some limitations in our study. This study has not considered the impact of human activities on runoff, as some studies have shown that changes in the QTP are mainly caused by climate change (Shi et al., 2022; Wang et al., 2018; Wang et al., 2021a, 2021b; Xu et al., 2021; Yi et al., 2021). Our results may slightly overestimate the contributions of precipitation and temperature to runoff change, and future research could consider the effect of human activities to obtain a more accurate attribution of runoff change. Despite these limitations, this study provides a comprehensive analysis of long-term runoff changes in the QTP over decades and offers insight into the attribution of runoff change.

6. Conclusions

This study conducted a systematic analysis of long-term changes in runoff and runoff coefficient on the QTP during 1961–2019 based on DTVGM and statistical methods. Furthermore, the study quantitatively estimated the relative contributions of precipitation and temperature to runoff change. The main findings of this study are as follows:

(1) The mean annual runoff over the QTP has a mean value of 184.77 mm (1961–2019), decreasing from the southeast (southern boundary of the plateau, 1605.97 mm) to the northwest (desert areas in the Inner basin, 1.76 mm). At the basin scale, the MJ, the NJ, and the DD have the highest mean annual runoff (median is 568.27 mm, 365.93 mm, and 359.20 mm, respectively), while the IN, the QL, and the JS have the lowest runoff (median is 79.29 mm, 121.96 mm, and 129.65 mm, respectively). Similarly, the mean annual runoff coefficient is high in the southeast and low in the northwest, with a mean value of 0.37. At the basin scale, the MJ has the highest runoff coefficient (median value is 0.63), while the JS and the IN are the lowest, with median values of 0.24 and 0.31, respectively.

(2) Interannual variations of runoff and runoff coefficient on the QTP both show significant increasing trends at rates of 9.13 mm/10 yr ($P < 0.001$) and 1.27 %/10 yr ($P < 0.001$), respectively. While the runoff on the QTP generally increases, the downstream YZ, the downstream NJ, and the northeastern IN show a decreasing trend. Similarly, the runoff coefficient shows declining trends in the downstream YZ, the downstream NJ, and the northeastern IN.

(3) The precipitation is a more important contributor than temperature, contributing 72.08 % and 27.92 % to the runoff change. At the basin scale, the influence of precipitation and temperature on runoff varies among basins. The IN is the least influenced by precipitation ($\overline{\eta_P}$ = 54.25 %), while the DD, the YR, and the YL are dominated by the influence of precipitation (the values of $\overline{\eta_P}$ are 99.03 %, 97.99 % and 96.01 %, respectively).

CRediT authorship contribution statement

Yunfei Wang: Data curation; Formal analysis; Methodology; Roles/Writing – original draft.

Aizhong Ye: Conceptualization; Data curation; Formal analysis; Funding acquisition; Writing – review & editing.

Yuhang Zhang: Data curation; Writing – review & editing.

Fan Yang: Validation; Writing – review & editing.

Data availability

Data will be made available on request.

Declaration of competing interest

The authors declare that they have no known competing financial interests or personal relationships that could have appeared to influence the work reported in this paper.

Acknowledgments

This study was supported by the Second Tibetan Plateau Scientific Expedition and Research Program (No. 2019QZK0405), the Natural Science Foundation of China (No. 42171022).

Appendix A. Supplementary data

Supplementary data to this article can be found online at https://doi.org/10.1016/j.scitotenv.2023.165326.

References

Box, G.E., 1953. Non-normality and tests on variances. Biometrika 40 (3/4), 318–335. https://doi.org/10.2307/2333350.

Chen, L., Liu, C., Li, Y., et al., 2007. Impacts of climatic factors on runoff coefficients in source regions of the Huanghe River. Chin. Geogr. Sci. 17, 047–055. https://doi.org/10.1007/s11769-007-0047-4.

Chen, B., Krajewski, W.F., Helmers, M.J., et al., 2019. Spatial variability and temporal persistence of event runoff coefficients for cropland hillslopes. Water Resour. Res. 55 (2), 1583–1597. https://doi.org/10.1029/2018WR023576.

Cui, T., Li, Y., Yang, L., Nan, Y., Li, K., Tudaji, M., et al., 2023. Non-monotonic changes in Asian Water Towers' streamflow at increasing warming levels. Nat. Commun. 14 (1), 1176. https://doi.org/10.1038/s41467-023-36804-6.

Du, C., Ye, A., Gan, Y., You, J., Duan, Q., Ma, F., et al., 2017. Drainage network extraction from a high-resolution DEM using parallel programming in the NET Framework. J. Hydrol. 555, 506–517. https://doi.org/10.1016/j.jhydrol.2017.10.034.

Gao, Y., Li, X., Leung, L.R., Chen, D., et al., 2015. Aridity changes in the Tibetan Plateau in a warming climate. Environ. Res. Lett. 10 (3), 034013. https://doi.org/10.1088/1748-9326/10/3/034013.

Guo, W., Liu, S., Xu, J., Wu, L., Shangguan, D., Yao, X., et al., 2015. The second Chinese glacier inventory: data, methods and results. J. Glaciol. 61 (226), 357–372. https://doi.org/10.3189/2015JoG14J209.

Han, P., Long, D., Han, Z., Du, M., Dai, L., et al., 2019. Improved understanding of snowmelt runoff from the headwaters of China's Yangtze River using remotely sensed snow products and hydrological modeling. Remote Sens. Environ. 224, 44–59. https://doi.org/10.1016/j.rse.2019.01.041.

Immerzeel, W.W., Van Beek, L.P., et al., 2010. Climate change will affect the Asian water towers. Science 328 (5984), 1382–1385. https://doi.org/10.1126/science.1183188.

Immerzeel, W.W., Lutz, A.F., Andrade, M., Bahl, A., Biemans, H., Bolch, T., et al., 2020. Importance and vulnerability of the world's water towers. Nature 577 (7790), 364–369. https://doi.org/10.1038/s41586-019-1822-y.

Jenson, S.K., Domingue, J.O., 1988. Extracting topographic structure from digital elevation data for geographic information system analysis. Photogramm. Eng. Remote. Sens. 54 (11), 1593–1600.

Kuang, X., Jiao, J.J., 2016. Review on climate change on the Tibetan Plateau during the last half century. J. Geophys. Res. Atmos. 121 (8), 3979–4007. https://doi.org/10.1002/2015JD024728.

Li, X., Long, D., Scanlon, B.R., Mann, M.E., Li, X., Tian, F., et al., 2022a. Climate change threatens terrestrial water storage over the Tibetan Plateau. Nat. Clim. Chang. 12 (9), 801–807. https://doi.org/10.1038/s41558-022-01443-0.

Li, M., Weng, B., Yan, D., Bi, W., Yang, Y., Gong, X., et al., 2022b. Spatiotemporal characteristics of surface water resources in the Tibetan plateau: based on the produce water coefficient method considering snowmelt. Sci. Total Environ. 851, 158048. https://doi.org/10.1016/j.scitotenv.2022.158048.

Lin, Z., Guojie, H., Defu, Z., Xiaodong, W.U., Lu, M.A., et al., 2019. Permafrost changes and its effects on hydrological processes on Qinghai-Tibet Plateau. Bull. Chin. Acad. Sci. 34 (11), 1233–1246. https://doi.org/10.16418/j.issn.1000-3045.2019.11.006 in Chinese.

Liu, Z., Yao, Z., Wang, R., et al., 2020. Estimation of the Qinghai-Tibetan Plateau runoff and its contribution to large Asian rivers. Sci. Total Environ. 749, 141570. https://doi.org/10.1016/j.scitotenv.2020.141570.

Lutz, A.F., Immerzeel, W.W., Shrestha, A.B., et al., 2014. Consistent increase in High Asia's runoff due to increasing glacier melt and precipitation. Nat. Clim. Chang. 4 (7), 587–592. https://doi.org/10.1038/nclimate2237.

Mahmood, R., Shaofeng, J.I.A., Lv, A., et al., 2020. A preliminary assessment of environmental flow in the three rivers' source region, Qinghai Tibetan Plateau, China and suggestions. Ecol. Eng. 144, 105709. https://doi.org/10.1016/j.ecoleng.2019.105709.

Mallakpour, I., Villarini, G., 2016. A simulation study to examine the sensitivity of the Pettitt test to detect abrupt changes in mean. Hydrol. Sci. J. 61 (2), 245–254. https://doi.org/10.1080/02626667.2015.1008482.

Merz, R., Blöschl, G., Parajka, J., 2006. Spatio-temporal variability of event runoff coefficients. J. Hydrol. 331 (3–4), 591–604. https://doi.org/10.1016/j.jhydrol.2006.06.008.

Peng, X., Frauenfeld, O.W., Jin, H., Du, R., Qiao, L., Zhao, Y., et al., 2021. Assessment of temperature changes on the Tibetan Plateau during 1980–2018. Earth Space Sci. 8 (4), e2020EA001609. https://doi.org/10.1029/2020EA001609.
Petrone, K.C., Hughes, J.D., Van Niel, T.G., et al., 2010. Streamflow decline in southwestern Australia, 1950–2008. Geophys. Res. Lett. 37 (11). https://doi.org/10.1029/2010GL043102.
Pettitt, A.N., 1979. A non-parametric approach to the change-point problem. J. R. Stat. Soc.: Ser. C: Appl. Stat. 28 (2), 126–135. https://doi.org/10.2307/2346729.
Shi, R., Wang, T., Yang, D., et al., 2022. Streamflow decline threatens water security in the upper Yangtze river. J. Hydrol. 606, 127448. https://doi.org/10.1016/j.jhydrol.2022.127448.
Sun, Q., Miao, C., et al., 2015. Projected changes in temperature and precipitation in ten river basins over China in 21st century. Int. J. Climatol. 35 (6), 1125–1141. https://doi.org/10.1002/joc.4043.
Wang, T., Yang, H., Yang, D., Qin, Y., et al., 2018. Quantifying the streamflow response to frozen ground degradation in the source region of the Yellow River within the Budyko framework. J. Hydrol. 558, 301–313. https://doi.org/10.1016/j.jhydrol.2018.01.050.
Wang, J., Chen, X., Liu, J., et al., 2021a. Changes of precipitation-runoff relationship induced by climate variation in a large Glaciated Basin of the Tibetan Plateau. J. Geophys. Res. Atmos. 126 (21), e2020JD034367. https://doi.org/10.1029/2020JD034367.
Wang, L., Yao, T., Chai, C., Cuo, L., Su, F., Zhang, F., et al., 2021b. TP-river: monitoring and quantifying total river runoff from the Third Pole. Bull. Am. Meteorol. Soc. 102 (5), E948–E965. https://doi.org/10.1175/BAMS-D-20-0207.1.
Xia, J., Wang, G.S., Lv, A.F., Tan, G., 2003. A research on distributed time variant gain modeling. Acta Geograph. Sin. 58 (5), 789–796 (in Chinese).
Xia, J., Wang, G., Tan, G., Ye, A., et al., 2005. Development of distributed time-variant gain model for nonlinear hydrological systems. Sci. China Ser. D Earth Sci. 48 (6), 713–723. https://doi.org/10.1360/03yd0183.
Xiong, J., Yin, J., Guo, S., He, S., Chen, J., 2022. Annual runoff coefficient variation in a changing environment: a global perspective. Environ. Res. Lett. 17 (6), 064006. https://doi.org/10.1088/1748-9326/ac62ad.
Xu, Z., Cheng, L., Liu, P., Makarieva, O., et al., 2021. Detecting and quantifying the impact of long-term terrestrial water storage changes on the runoff ratio in the head regions of the two largest rivers in China. J. Hydrol. 601, 126668. https://doi.org/10.1016/j.jhydrol.2021.126668.
Yao, T., 2019. Tackling on environmental changes in Tibetan Plateau with focus on water, ecosystem and adaptation. Sci. Bull. 64 (7), 417. https://doi.org/10.1016/j.scib.2019.03.033.
Yao, T., Thompson, L., Yang, W., Yu, W., Gao, Y., Guo, X., et al., 2012. Different glacier status with atmospheric circulations in Tibetan Plateau and surroundings. Nat. Clim. Chang. 2 (9), 663–667. https://doi.org/10.1038/nclimate1580.
Yao, T., Wu, G., Xu, B., et al., 2019a. Asian water tower change and its impacts. Bull. Chin. Acad. Sci. 34 (11), 1203–1209. https://doi.org/10.16418/j.issn.1000-3045.2019.11.003 in Chinese.
Yao, T., Xue, Y., Chen, D., Chen, F., Thompson, L., Cui, P., et al., 2019b. Recent third pole's rapid warming accompanies cryospheric melt and water cycle intensification and interactions between monsoon and environment: multidisciplinary approach with observations, modeling, and analysis. Bull. Am. Meteorol. Soc. 100 (3), 423–444. https://doi.org/10.1175/BAMS-D-17-0057.1.
Yao, T., Bolch, T., Chen, D., Gao, J., Immerzeel, W., Piao, S., et al., 2022. The imbalance of the Asian water tower. Nat. Rev. Earth Environ. 3 (10), 618–632. https://doi.org/10.1038/s43017-022-00299-4.
Ye, A., Xia, J., Wang, G., et al., 2005. Drainage network extraction and subcatchment delineation based on digital elevation model. J. Hydraul. Eng. 05, 531–537. https://doi.org/10.13243/j.cnki.slxb.2005.05.00 (in Chinese).
Ye, A., Duan, Q., Zeng, H., et al., 2010. A distributed time-variant gain hydrological model based on remote sensing. J. Resour. Ecol. 1 (3), 222–230. https://doi.org/10.3969/j.issn.1674-764x.2010.03.005.
Ye, A., Duan, Q., Zhan, C., Liu, Z., Mao, Y., 2013. Improving kinematic wave routing scheme in community land model. Hydrol. Res. 44 (5), 886–903. https://doi.org/10.2166/nh.2012.145.
Yi, W., Feng, Y., Liang, S., Kuang, X., Yan, D., et al., 2021. Increasing annual streamflow and groundwater storage in response to climate warming in the Yangtze River source region. Environ. Res. Lett. 16 (8), 084011. https://doi.org/10.1088/1748-9326/ac0f27.
Zhang, L., Dawes, W.R., et al., 2001. Response of mean annual evapotranspiration to vegetation changes at catchment scale. Water Resour. Res. 37 (3), 701–708. https://doi.org/10.1029/2000WR900325.
Zhang, L., Nan, Z., Wang, W., Ren, D., Zhao, Y., et al., 2019a. Separating climate change and human contributions to variations in streamflow and its components using eight time-trend methods. Hydrol. Process. 33 (3), 383–394. https://doi.org/10.1002/hyp.13331.
Zhang, G., Nan, Z., Wu, X., Ji, H., Zhao, S., 2019b. The role of winter warming in permafrost change over the Qinghai-Tibet Plateau. Geophys. Res. Lett. 46 (20), 11261–11269. https://doi.org/10.1029/2019GL084292.
Zhang, Y., Ye, A., You, J., et al., 2021. Quantification of human and climate contributions to multi-dimensional hydrological alterations: a case study in the Upper Minjiang River, China. J. Geogr. Sci. 31 (8), 1102–1122. https://doi.org/10.1007/s11442-021-1887-z.
Zhao, Q., Ding, Y., Wang, J., Gao, H., Zhang, S., Zhao, C., et al., 2019. Projecting climate change impacts on hydrological processes on the Tibetan Plateau with model calibration against the glacier inventory data and observed streamflow. J. Hydrol. 573, 60–81. https://doi.org/10.1016/j.jhydrol.2019.03.043.
Zheng, H., Miao, C., Zhang, G., Li, X., Wang, S., Wu, J., et al., 2021. Is the runoff coefficient increasing or decreasing after ecological restoration on China's Loess Plateau? Int. Soil Water Conserv. Res. 9 (3), 333–343. https://doi.org/10.1016/j.iswcr.2021.04.009.